SCIENTIFIC REPORTS

OPEN

Received: 12 January 2016
Accepted: 31 March 2016
Published: 18 April 2016

Sensitive Electrochemical Immunosensor for Detection of Nuclear Matrix Protein-22 based on NH_2-SAPO-34 Supported Pd/Co Nanoparticles

Dan Wu[1], Yaoguang Wang[1], Yong Zhang[1], Hongmin Ma[1], Tao Yan[2], Bin Du[2] & Qin Wei[1]

A novel sandwich-type electrochemical immunosensor using the new amino group functionalized silicoaluminophosphates molecular sieves (NH_2-SAPO-34) supported Pd/Co nanoparticles (NH_2-SAPO-34-Pd/Co NPs) as labels for the detection of bladder cancer biomarker nuclear matrix protein-22 (NMP-22) was developed in this work. The reduced graphene oxide-NH (rGO-NH) with good conductivity and large surface area was used to immobilize primary antibody (Ab_1). Due to the excellent catalytic activity toward hydrogen peroxide, NH_2-SAPO-34-Pd/Co NPs were used as labels and immobilized secondary antibody (Ab_2) through adsorption capacity of Pd/Co NPs to protein. The immunosensor displayed a wide linear range (0.001–20 ng/mL) and low detection limit (0.33 pg/mL). Good reproducibility and stability have showed satisfying results in the analysis of clinical urine samples. This novel and ultrasensitive immunosensor may have the potential application in the detection of different tumor markers.

Bladder cancer (BC) is one of the most common urinary cancers[1]. For the clinical diagnosis of human bladder cancer, cystoscopy is considered to be the gold standard[2,3]. However, the cystoscopy is expensive, invasive[4,5] and it has difficulties in detecting upper urinary tract lesions. Therefore, it is necessary to develop a noninvasive, quick and highly sensitive method for the detection of BC. Nuclear matrix protein-22 (NMP-22) is a nuclear mitotic apparatus protein which is involved in the proper distribution of chromatids to daughter cells during cellular replication[6–8]. NMP-22 is widely used as a tumor marker for bladder tumor, and is involved with DNA recombination and replication, RNA transcription and mitosis[5,9,10]. Numerous studies show that the level of NMP-22 is usually less than 5 ng/mL, and 80% of terminal bladder cancer people have high levels of NMP-22[11,12]. NMP-22 is thought to be an objective, noninvasive, quantitative test with good accuracy in BC diagnosis, especially for low-grade tumors[12,13]. NMP-22 has become increasingly significant in the detection of bladder cancer and is being used for the diagnosis and detection of recurrence[13].

Reduced graphene oxide (rGO), a two-dimensional nanomaterial consisted of sp^2-hybridized carbon atoms to form a one-atom thick honeycomb lattice, has been considered as a promising candidate for electron-acceptor and electron-transfer material due to its excellent optical and electrical properties, which has been extensively studied in the field of electrochemical immunoassay[14–18]. Moreover, the populated chemical moieties on the rGO surface offer the convenience and flexibility for various functionalizations to enhance the sensor performance. More importantly, rGO may also be functionalized through covalent or non-covalent methods in order to further enhance its sensitivity, specificity, loading capacity, biocompatibility, etc. Reduced graphene oxide-NH (rGO-NH) is a novel material which is a combination of rGO and piperazine through covalent bonding. The rGO-NH not only keeps the original property of rGO but also promotes water solubility.

[1]Key Laboratory of Chemical Sensing & Analysis in Universities of Shandong, School of Chemistry and Chemical Engineering, University of Jinan, Jinan 250022, P.R. China. [2]School of Resources and Environment, University of Jinan, Jinan 250022, P.R. China. Correspondence and requests for materials should be addressed to Q.W. (email: sdjndxwq@163.com)

Ordered mesoporous materials are one kind of molecular sieve which have attracted increasing interest owing to the unique properties which can be effectively applied in electrochemical devices[19], the fields of catalysis and supported catalysts[20–22], electroanalytical chemistry[23–27] and biosensors[28–31]. The silicoaluminophosphates molecular sieves (SAPO-34) with high stability, microporosity, large specific surface area and acid sites[32–35] can immobilize more Pd/Co nanoparticles and enhance the sensitivity of immunosensor. Pd-based catalysts have been widely used as catalysts for the direct synthesis of hydrogen peroxide (H_2O_2) from oxygen and hydrogen elemental[36,37], and the decomposition of H_2O_2 is also catalyzed by Pd-based catalysts[38,39]. However, Pd/Co nanoparticles have not been studied for designing electrochemical immunosensor. In this work, the novel amino group functionalized silicoaluminophosphates molecular sieves (NH_2-SAPO-34) supported Pd/Co nanoparticles (NH_2-SAPO-34-Pd/Co NPs) were first used as labels of the secondary antibody (Ab_2).

In this work, a sandwich-type electrochemical immunosensor for the detection of NMP-22 was prepared by using NH_2-SAPO-34-Pd/Co NPs as labels and rGO-NH as sensing platform for the signal amplification. The large surface area of rGO-NH could increase the loading of Ab_1 and the good conductivity of rGO-NH could promote the electron transfer. The high catalysis of NH_2-SAPO-34-Pd/Co NPs toward the reduction of H_2O_2 could improve the sensitivity of the immunosensor. Therefore, this simple, economic and sensitive immunosensor could be widely used in the clinical analysis.

Experimental

Materials and reagents. NMP-22 antigen and antibody were purchased from Guyan Biotech Co., Ltd. (Shanghai, China). $K_3[Fe(CN)_6]$ was purchased from Sinopharm Chemical Reagent Co., Ltd. Glutaraldehydes (GA) and sodium tetrachloropalladate (Na_2PdCl_4) were purchased from Sinopharm Chemical Reagent Beijing Co., Ltd. (China). Cobalt nitrate was obtained from Shanghai Chemical Reagent Plant (China). Bovine serum albumin (BSA) and chitosan (CS) were purchased from Sigma-Aldrich. The rGO-NH was obtained from Nano Innova Technologies Co., Ltd. (Spain)[40]. The SAPO-34 was purchased from the catalyst factory of Nankai University (China). Phosphate buffered saline (PBS, 1/15 M Na_2HPO_4 and KH_2PO_4) was used as electrolyte for all electrochemical measurement. Ultrapure water was used throughout the experiments.

Apparatus. All electrochemical measurements were performed on a CHI760D electrochemical workstation (Shanghai CH Instruments Co., China). Scanning electron microscope (SEM) and Energy Dispersive X-Ray Spectroscopy (EDS) were recorded by JEOL JSM-6700F microscope (Japan). A conventional three-electrode system was used for all electrochemical measurements: the modified glassy carbon electrode (GCE, 4 mm in diameter) as the working electrode, a saturated calomel electrode (SCE) as the reference electrode, and platinum wire electrode as the counter electrode.

Preparation of NH_2-SAPO-34. 0.1 g of SAPO-34 powder, 0.1 mL of 3-ammonia propyl triethoxy silane and 10 mL of anhydrous ethanol were added into the three necked flask, the mixture was heated to and kept at 70 °C for 1.5 h. Then the product was cooled down to room temperature and collected by centrifugation (7000 rpm, 5 min). Finally, the product was collected after washing and drying in vacuum at 40 °C.

Synthesis of NH_2-SAPO-34-Pd/Co NPs. The NH_2-SAPO-34-Pd/Co NPs were synthesized by a modified two-step reduction route under the protection of high-purity nitrogen in an ice bath[41]. Firstly, 4 mL of 0.2 mol/L $Co(NO_3)_2$, 2.5 mL of 64 mmol/L sodium citrate, 30 mg of NH_2-SAPO-34 and 25 mL of ultrapure water were mixed ultrasonically for 20 min. Then, 5 mL of 1.6 mol/L $NaBH_4$ solution was added into the above mixture at a rate of 20 mL/h under vigorous stirring to generate the Co NPs. Secondly, 10 mL of 40 mmol/L Na_2PdCl_4 solution and 10 mL of 0.16 mol/L $NaBH_4$ solution were synchronously added into the solution of Co NPs at a rate of 20 mL/h. Finally, the resulting NH_2-SAPO-34-Pd/Co NPs was filtrated, washed with ultra-pure water for more than three times and then dried in vacuum at 35 °C.

Preparation of NH_2-SAPO-34-Pd/Co-Ab_2. The NH_2-SAPO-34-Pd/Co-Ab_2 was synthesized by the following steps (Fig. 1(a)). A solution of NH_2-SAPO-34-Pd/Co NPs (2 mg/mL, 1 mL) was added into Ab_2 dispersion (10 μg/mL, 1 mL) and stirred for 12 h at 4 °C. After centrifugation, the resulting NH_2-SAPO-34-Pd/Co-Ab_2 was dispersed in 1 mL of PBS at pH 7.0 and stored at 4 °C.

Modification of electrodes. Figure 1(b) showed the fabrication procedure of the immunosensor. A glassy carbon electrode was polished to a mirror-like finish with 1.0, 0.3 and 0.05 μm alumina powder and then thoroughly cleaned. Afterwards, 6.0 μL of rGO-NH solution (1.5 mg/mL) dispersed in chitosan (0.1 wt%) was dropped onto the electrode surface and then dried at room temperature. The utilization of chitosan could make rGO-NH forming a film on the electrode surface and the abundant amino groups in CS could provide active sites for Ab_1 immobilization. To immobilize the Ab_1 onto the electrode, 3.0 μL of GA (2.5%, v/v) was dropped onto the electrode surface and incubated until it was half-dry. Then, 6.0 μL of Ab_1 (10 μg/mL) was dropped onto the electrode surface and then incubated for 1 h. In this procedure, GA was used as cross-linking agent to link amino groups of antibody with amino groups of CS. After drying, the electrode was incubated in 1 wt% BSA solution for another 30 min to eliminate nonspecific binding sites. Subsequently, NMP-22 solution with different concentrations were dropped onto the electrode surface and incubated for 1 h, and the excess antigen was rinsed away with water. Finally, 6.0 μL of the prepared NH_2-SAPO-34-Pd/Co-Ab_2 solution was dropped onto the electrode surface and bound to NMP-22 via the specific antibody-antigen interaction. After incubation, the electrode was then rinsed and stored at 4 °C before use. The label NH_2-SAPO-34-Pd/Co could catalyze the reduction of H_2O_2, so that different current response could be generated in accordance with NMP-22 concentration when 10 μL of H_2O_2 (5.0 mol/L) was added into 10 mL of PBS under magnetic stirring.

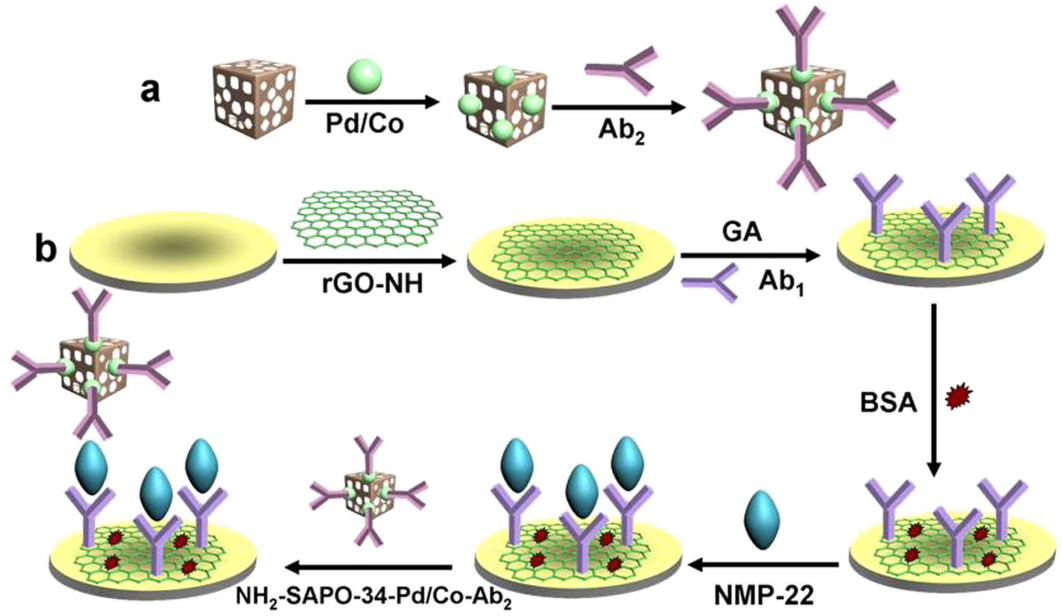

Figure 1. Schematic representation of the preparation of the NH_2-SAPO-34-Pd/Co-Ab_2 (**a**) and fabrication process of modified immunosensor (**b**).

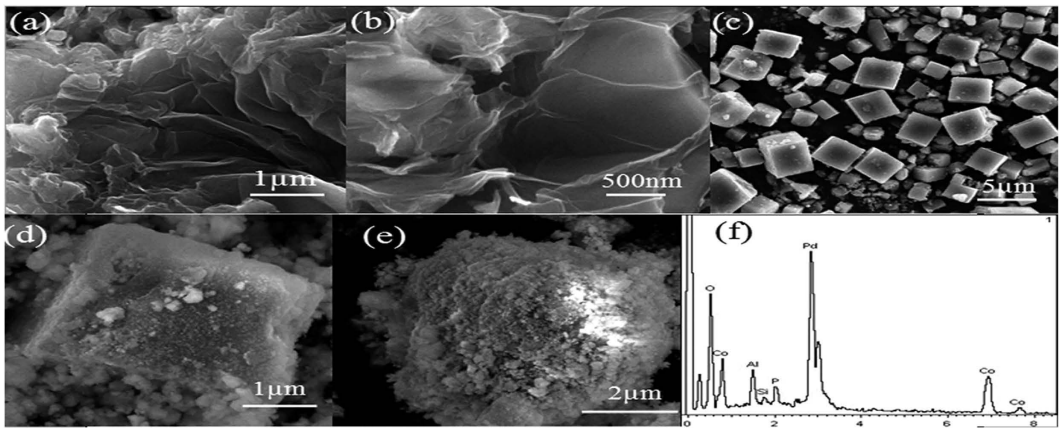

Figure 2. SEM images of rGO-NH (**a,b**) NH_2-SAPO-34 (**c**) and NH_2-SAPO-34-Pd/Co NPs (**d,e**); EDS of NH_2-SAPO-34-Pd/Co NPs (**f**).

Results and Discussion

Characterization of rGO-NH and NH_2-SAPO-34-Pd/Co NPs. The rGO-NH with large surface area was used to increase the amount of captured Ab_1. The SEM images (Fig. 2a,b) of the rGO-NH showed that the rGO-NH had a wrinkle paper-like structure with irregular size, further indicating the large surface area of rGO-NH. The SEM image of NH_2-SAPO-34 was shown in Fig. 2c, which showed the NH_2-SAPO-34 possessed cubic structure. The NH_2-SAPO-34 had a BET surface area of 536.6 m^2/g. Due to the large surface area, more Pd/Co nanoparticles could be loaded on the surface of NH_2-SAPO-34 and the SEM images (Fig. 2d,e) of NH_2-SAPO-34-Pd/Co presented that the NH_2-SAPO-34 was coated successfully. Elemental compositions of NH_2-SAPO-34-Pd/Co NPs were analyzed by EDS (Fig. 2f). Signature peaks of Si, O, P, Al, Pd and Co were observed, indicating that the Pd/Co nanoparticles were formed successfully on the surface of NH_2-SAPO-34.

Characterization of NH_2-SAPO-34-Pd/Co NPs modified electrode. The performance of NH_2-SAPO-34-Pd/Co toward the H_2O_2 reduction was investigated (Fig. 3). As shown, the electrode modified by NH_2-SAPO-34-Pd/Co-Ab_2 exhibited obvious current change toward H_2O_2. However, the electrode did not appear to be electroactive toward water. The NH_2-SAPO-34-Pd/Co NPs showed the ability to promote the reduction of H_2O_2 and resulted in the generation of electrochemical signals.

Characterization of the immunosensor. The stepwise modified process of electrode was characterized by cyclic voltammetry (CV). CV can also characterize the modification process of the immunosensor besides electrochemical impedance spectroscopy, and each immobilization step was shown in Fig. 4. It could be seen that

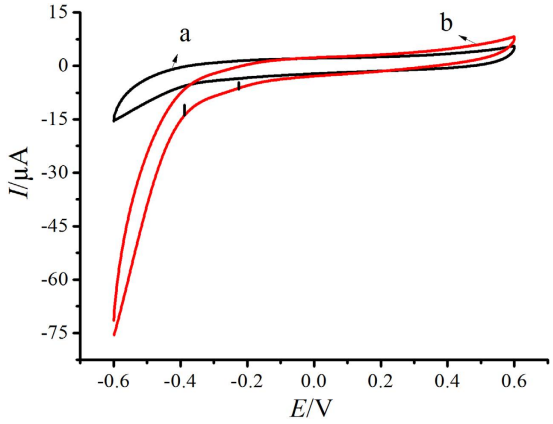

Figure 3. Cyclic voltammograms of electrode modified by NH_2-SAPO-34-Pd/Co-Ab_2 (2 mg/mL) in N_2-saturated PBS without (**a**) and with (**b**) 5.0 mmol/L H_2O_2.

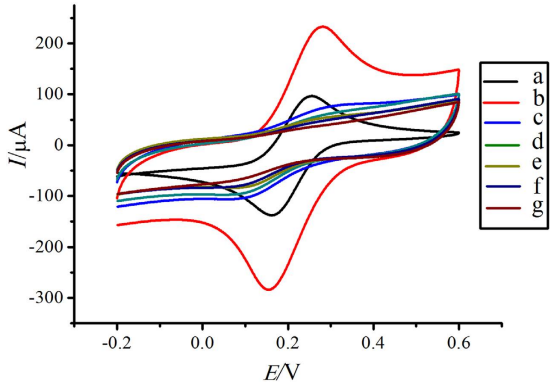

Figure 4. The cyclic voltammetry for each immobilized step in a PBS of pH 7.0 buffer solution containing 5 mmol/L $K_3[Fe(CN)_6]$ on the response of the immunosensor to 10 ng/mL NMP-22. The bare GCE (**a**), rGO-NH/GCE (**b**), GA/rGO-NH/GCE (**c**), Ab_1/GA/rGO-NH/GCE (**d**), BSA/Ab_1/GA/rGO-NH/GCE (**e**), NMP-22/BSA/Ab_1/GA/rGO-NH/GCE (**f**) and NH_2-SAPO-34-Pd/Co-Ab_2/NMP-22/BSA/Ab_1/GA/rGO-NH/GCE (**g**).

a pair of well-defined redox peak was observed on GCE (curve a), and this quasi-reversible one-electron redox peak was attributed to the transformation between $Fe(CN)_6^{4-}$ and $Fe(CN)_6^{3-}$. The redox peak current increased strongly after rGO-NH was dropped onto the electrode surface (curve b), which suggested the rGO-NH had good conductivity and strong ability of electron transfer. The redox peak current decreased significantly after GA was dropped onto the rGO-NH modified electrode (curve c), which could be attributed to the large impedence of GA. The redox peak current decreased gradually when Ab_1 (curve d), BSA (curve e) and NMP-22 (curve f) as the non-conductive bioactive substances were modified layer by layer on the electrode. The results suggested that the non-conductive bioactive substances were immobilized onto the electrode successfully and blocked electron exchange between the redox probe and the electrode. The redox peak current decreased to the minimum (curve g) when NH_2-SAPO-34-Pd/Co-Ab_2 were immobilized, indicated the formation of hydrophobic immunocomplex layer could embarrass electron transfer. As a result, the immunosensor was modified successfully.

Optimization of experimental conditions. To achieve an optimal electrochemical signal, the influence of the pH value of substrate solution to the immunosensor was investigated at first. Herein, 6.0 μL of rGO-NH solution (1.5 mg/mL) dispersed in chitosan (0.1 wt%) was dropped onto the electrode surface. Then the same amount of Ab_1 (6.0 μL, 10 μg/mL) and NMP-22 (6.0 μL, 10 ng/mL) were used to fabricate the immunosensors. As shown in Fig. 5(a), it could be found that the current response increased with increasing pH value from 5.8 to 7.0 to reach the maximum and decreased from 7.0 to 7.9. The reason is that the highly acidic or alkaline surroundings would damage the activity of immobilized protein[42]. Therefore, pH 7.0 PBS was selected for the test throughout this study.

Apart from the pH value of substrate solution, the concentration of rGO-NH was also an important parameter, which could affect not only the loading of captured antibody (Ab_1) but also the electrochemical behaviors of the rGO-NH modified electrode. In detail, different concentrations of rGO-NH from 0.5 mg/mL to 2.0 mg/mL with the same amount of Ab_1 (6.0 μL, 10 μg/mL) and NMP-22 (6.0 μL, 10 ng/mL) were employed to modify the electrodes. As seen in Fig. 5(b), with the increasing concentration of rGO-NH, the current response for detection of 10 ng/mL NMP-22 increased due to the enhanced loading of Ab_1 for bound more antigens and then

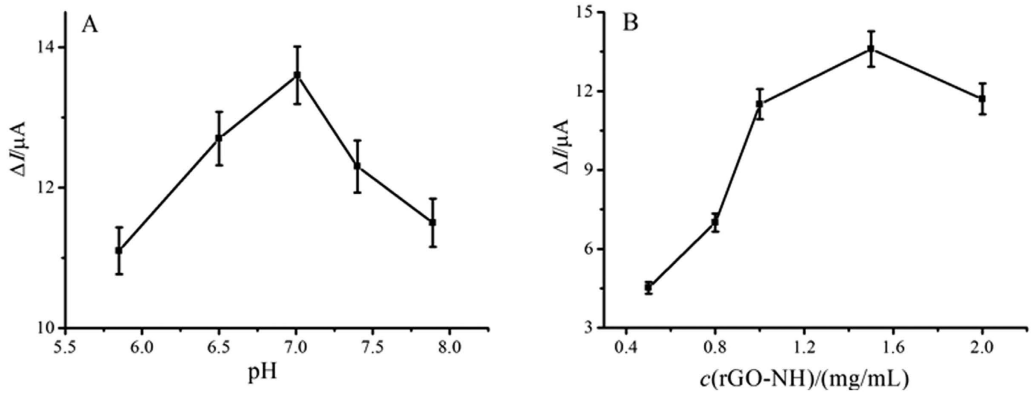

Figure 5. (**a**) Effect of pH ($C_{rGO\text{-}NH}$ = 1.5 mg/mL, pH = 5.85, 6.50, 7.00, 7.40 and 7.89) and (**b**) the concentration of rGO-NH (pH = 7.0, $C_{rGO\text{-}NH}$ = 0.5, 0.8, 1.0, 1.5 and 2.0 mg/mL) on the response of the immunosensor to 10 ng/mL NMP-22. Error bar = RSD (n = 5).

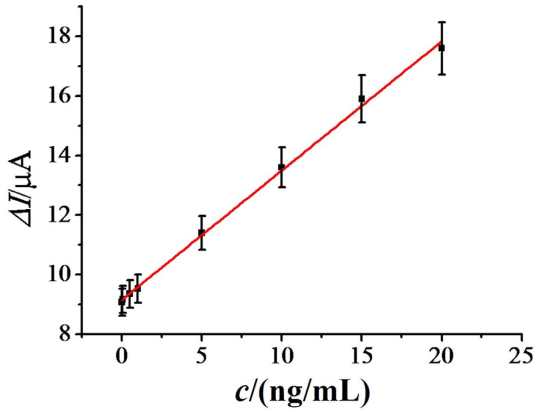

Figure 6. Calibration curve of the immunosensor toward different concentrations of NMP-22 (0.001, 0.05, 0.5, 1, 5, 10, 15, 20 ng/mL). Error bar = RSD (n = 5).

Methods	Linear range	Detection limit	Reference
Electrochemical immuno-biosensor	1.2–200 ng/mL	0.5 ng/mL	43
Electrochemical sensing	128–588 ng/mL	–	44
Label-free electrochemiluminescence immunosensor	0.05–2.0 ng/mL	10.0 pg/mL	45
Electrochemical immunosensor	0.001–20 ng/mL	0.33 pg/mL	This work

Table 1. Comparisons of proposed method with other reports for NMP-22.

NH_2-SAPO-34-Pd/Co-Ab_2. However, when the concentration of the rGO-NH was more than 1.5 mg/mL, the current response decreased. Therefore, the optimal concentration of rGO-NH solution was 1.5 mg/mL.

Under the optimum conditions, the immunosensors using NH_2-SAPO-34-Pd/Co NPs as labels were prepared for the detection of different concentrations of NMP-22 in pH 7.0 PBS at −0.4 V. The relationship between the current response toward 5.0 mmol/L H_2O_2 and NMP-22 concentration was shown in Fig. 6. As can be seen, the current response increased linearly with the increasing concentration of the NMP-22 in the range from 0.001 to 20 ng/mL, with a detection limit of 0.33 pg/mL based on S/N = 3. The detection limit of this immunosensor is significantly lower than other methods[43–45], as shown in Table 1. The calibration curve was linear with a correlation coefficient of $R^2 = 0.998$ ($\Delta I = 0.434\, c + 9.16$).

To the further development of techniques, lower limit of detection is a major criterion of successful application. The low detection limit may be attributed to three factors: (1) The rGO-NH with large surface area could greatly increase the loading of Ab_1 and promote electrons transfer because of its good conductivity; (2) SAPO-34 molecular sieves with large surface area could increase the loading of Pd/Co nanoparticles, which means more Ab_2 could be loaded onto the label; (3) The good catalytic activity of NH_2-SAPO-34-Pd/Co-Ab_2 toward H_2O_2 could increase the sensitivity of the immunosensor. Hence, the proposed strategy could provide a stable immobilization and sensitized recognition platform for analytes such as micromolecules and possesses promising application in clinical sample.

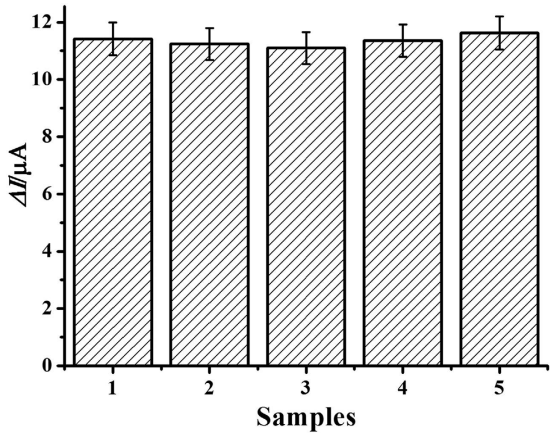

Figure 7. Amperometric response of the immunosensor to 5 ng/mL NMP-22 (1), 5 ng/mL NMP-22 + 500 ng/mL BSA (2), 5 ng/mL NMP-22 + 500 ng/mL vitamin C (3), 5 ng/mL NMP-22 + 500 ng/mL trioxypurine (4), 5 ng/mL NMP-22 + 500 ng/mL glucose (5). Error bar: RSD ($n = 5$).

Urine Sample	Content of NMP-22 (ng/mL)	Added (ng/mL)	Found (n = 5 ng/mL)	RSD (%, n = 5)	Recovery (%, n = 5)
1	2.99	5.00	7.79 8.11 8.05 7.87 7.95	1.6	99.5
2	0.73	3.00	4.12 3.79 3.50 3.63 3.84	6.2	101.2

Table 2. Results for the determination of NMP-22 in the clinical urine sample by the immunosensor.

Reproducibility, selectivity and stability. To evaluate the reproducibility of the immunosensor, a series of five electrodes were prepared for the detection of NMP-22 (5 ng/mL). The results of the measurements were 11.7, 11.1, 11.9, 10.8 and 11.0 μA, respectively. The relative standard deviation (RSD) of the measurements for the five electrodes was 4.2%, suggesting the precision and reproducibility of the proposed immunosensor were good.

The selectivity of the immunosensor was also investigated. Interferences study was performed by using bovine serum albumin (BSA), vitamin C, trioxypurine and glucose. NMP-22 (5 ng/mL) solutions containing 500 ng/mL of interfering substances were measured by the immunosensor. The results were shown in Fig. 7. The current variation due to the interfering substances was less than 5.0% of that without interferences, indicating that the selectivity of the immunosensor was acceptable.

Stability of the immunosensor is also a key factor in their application and development. The stability of the immunosensor for 5 ng/mL NMP-22 was examined by checking periodically its current response. When the immunosensor was not used, it was stored at 4 °C. After ten days, the current of the immunosensor retained about 97% of its initial value. The good long-term stability may be ascribed to the good stability of the NH_2-SAPO-34-Pd/Co and rGO-NH.

Real sample analysis. To evaluate the potential of this immunosensor for real sample analysis, the practical detection for two urine samples covered by the calibration curve is further conducted. As shown in Table 2, the RSD between 1.6% and 6.2% were obtained. The recovery was in the range from 99.5% to 101.2%. Therefore, the immunosensor could be used in the clinical analysis.

Conclusion

The large surface area of rGO-NH could increase the amount of Ab_1 immobilized on the electrode surface and the good conductivity of rGO-NH could promote the electrons transfer. The NH_2-SAPO-34 supported Pd/Co nanoparticles showed high catalysis toward the reduction of H_2O_2, which improve the sensitivity of the immunosensor. The immunosensor has adequate sensitivity and precision, with wide linear range and low detection limit of 0.33 pg/mL. Due to the advantages of simplicity, high selectivity and good reproducibility, this new immunosensor may have the potential application in the detection of different cancer biomarkers.

References

1. Chang, Y.-H. *et al.* Evaluation of nuclear matrix protein-22 as a clinical diagnostic marker for bladder cancer. *Urology* **64,** 687–692 (2004).
2. Dey, P. Urinary markers of bladder carcinoma. *Clin. Chim. Acta* **340,** 57–65 (2004).
3. Pasikanti, K. K. *et al.* Noninvasive urinary metabonomic diagnosis of human bladder cancer. *J. Proteome Res.* **9,** 2988–2995 (2010).
4. Botteman, M. F., Pashos, C. L., Redaelli, A., Laskin, B. & Hauser, R. The health economics of bladder cancer. *Pharmacoeconomics* **21,** 1315–1330 (2003).
5. Hwang, E. C. *et al.* Use of the NMP22 BladderChek test in the diagnosis and follow-up of urothelial cancer: a cross-sectional study. *Urology* **77,** 154–159 (2011).

6. Berezney, R. & Coffey, D. S. Identification of a nuclear protein matrix. *Biochem. Bioph. Res. Co.* **60,** 1410–1417 (1974).
7. Yang, C. H., Lambie, E. J. & Snyder, M. NuMA: an unusually long coiled-coil related protein in the mammalian nucleus. *J. Cell Biol.* 116, 1303–1317 (1992).
8. Compton, D. A. & Cleveland, D. W. NuMA is required for the proper completion of mitosis. *J. Cell Biol.* **120,** 947–957 (1993).
9. Pardoll, D. M., Vogelstein, B. & Coffey, D. S. A fixed site of DNA replication in eucaryotic cells. *Cell* **19,** 527–536 (1980).
10. Gordon, J. N., Shu, W.-P., Schlussel, R. N., Droller, M. J. & Liu, B. C. Altered extracellular matrices influence cellular processes and nuclear matrix organizations of overlying human bladder urothelial cells. *Cancer Res.* **53,** 4971–4977 (1993).
11. Shariat, S. F. *et al.* Variability in the performance of nuclear matrix protein 22 for the detection of bladder cancer. *J. Urology* **176,** 919–926 (2006).
12. Miyanaga, N. *et al.* Clinical evaluation of nuclear matrix protein 22 (NMP22) in urine as a novel marker for urothelial cancer. *Eur. Urol.* **31,** 163–168 (1997).
13. Menendez, V. *et al.* Usefulness of urinary nuclear matrix protein 22 (NMP22) as a marker for transitional cell carcinoma of the bladder. *Anticancer Res.* **20,** 1169–1172 (2000).
14. Shangguan, L., Zhu, W., Xue, Y. & Liu, S. Construction of photoelectrochemical thrombin aptasensor via assembling multilayer of graphene-CdS nanocomposites. *Biosens. Bioelectron.* **64,** 611–617 (2015).
15. Huang, J. *et al.* An electrochemical impedimetric immunosensor for label-free detection of Campylobacter jejuni in diarrhea patients' stool based on O-carboxymethylchitosan surface modified Fe_3O_4 nanoparticles. *Biosens. Bioelectron.* **25,** 1204–1211 (2010).
16. Lu, J., Cui, D., Li, H., Zhang, Y. & Liu, S. Cytochrome P450 bienzymes assembled on Au/chitosan/reduced graphene oxide nanosheets for electrochemically-driven drug cascade metabolism. *Electrochim. Acta* **165,** 36–44 (2015).
17. Sun, B., Zhang, K., Chen, L., Guo, L. & Ai, S. A novel photoelectrochemical sensor based on PPIX-functionalized WO_3–rGO nanohybrid-decorated ITO electrode for detecting cysteine. *Biosens. Bioelectron.* **44,** 48–51 (2013).
18. Teymourian, H., Salimi, A. & Khezrian, S. Fe_3O_4 magnetic nanoparticles/reduced graphene oxide nanosheets as a novel electrochemical and bioeletrochemical sensing platform. *Biosens. Bioelectron.* **49,** 1–8 (2013).
19. Lin, J., He, C. & Zhang, S. Immunoassay channels for α-fetoprotein based on encapsulation of biorecognition molecules into SBA-15 mesopores. *Anal. Chim. Acta* **643,** 90–94 (2009).
20. Taguchi, A. & Schüth, F. Ordered mesoporous materials in catalysis. *Micropor. Mesopor. Mat.* **77,** 1–45 (2005).
21. Clark, J. H., Macquarrie, D. J. & Tavener, S. J. The application of modified mesoporous silicas in liquid phase catalysis. *Dalton T.* **36,** 4297–4309 (2006).
22. Gabaldon, J. P., Bore, M. & Datye, A. K. Mesoporous silica supports for improved thermal stability in supported Au catalysts. *Top. Catal.* **44,** 253–262 (2007).
23. Walcarius, A. & Collinson, M. M. Analytical chemistry with silica sol-gels: traditional routes to new materials for chemical analysis. *Ann. Rev. Anal. Chem.* **2,** 121–143 (2009).
24. Walcarius, A., Mandler, D., Cox, J. A., Collinson, M. & Lev, O. Exciting new directions in the intersection of functionalized sol-gel materials with electrochemistry. *J. Mater. Chem.* **15,** 3663–3689 (2005).
25. Walcarius, A. & Kuhn, A. Ordered porous thin films in electrochemical analysis. *TrAC-Trend. Anal. Chem.* **27,** 593–603 (2008).
26. Walcarius, A. Template-directed porous electrodes in electroanalysis. *Anal. Bioanal. Chem.* **396,** 261–272 (2010).
27. Walcarius, A. Electrocatalysis, sensors and biosensors in analytical chemistry based on ordered mesoporous and macroporous carbon-modified electrodes. *TrAC-Trend. Anal. Chem.* **38,** 79–97 (2012).
28. Walcarius, A. Electroanalytical applications of microporous zeolites and mesoporous (organo) silicas: recent trends. *Electroanal.* **20,** 711–738 (2008).
29. Slowing, I. I., Trewyn, B. G., Giri, S. & Lin, V. Y. Mesoporous silica nanoparticles for drug delivery and biosensing applications. *Adv. Funct. Mater.* **17,** 1225–1236 (2007).
30. Ispas, C., Sokolov, I. & Andreescu, S. Enzyme-functionalized mesoporous silica for bioanalytical applications. *Anal. Bioanal. Chem.* **393,** 543–554 (2009).
31. Hasanzadeh, M., Shadjou, N., Eskandani, M. & de la Guardia, M. Mesoporous silica-based materials for use in electrochemical enzyme nanobiosensors. *TrAC-Trend. Anal. Chem.* **40,** 106–118 (2012).
32. Pastore, H., Coluccia, S. & Marchese, L. Porous aluminophosphates: from molecular sieves to designed acid catalysts. *Annu. Rev. Mater. Res.* **35,** 351–395 (2005).
33. Hartmann, M. & Kevan, L. Transition-metal ions in aluminophosphate and silicoaluminophosphate molecular sieves: location, interaction with adsorbates and catalytic properties. *Chem. Rev.* **99,** 635–664 (1999).
34. Maxwell, I. Zeolite catalysis in hydroprocessing technology. *Catal. Today* **1,** 385–413 (1987).
35. Dai, P.-S. E. Zeolite catalysis for a better environment. *Catal. Today* **26,** 3–11 (1995).
36. Choudhary, V., Samanta, C. & Choudhary, T. Direct oxidation of H_2 to H_2O_2 over Pd-based catalysts: Influence of oxidation state, support and metal additives. *Appl. Catal. A-Gen.* **308,** 128–133 (2006).
37. Liu, Q. & Lunsford, J. H. Controlling factors in the direct formation of H_2O_2 from H_2 and O_2 over a Pd/SiO_2 catalyst in ethanol. *Appl. Catal. A-Gen.* **314,** 94–100 (2006).
38. Moreno, T., García-Serna, J. & Cocero, M. J. Decomposition reaction of H_2O_2 over Pd/C catalyst in an aqueous medium at high pressure: detailed kinetic study and modelling. *J. Supercrit. Fluid.* **57,** 227–235 (2011).
39. Choudhary, V. R., Samanta, C. & Choudhary, T. Factors influencing decomposition of H_2O_2 over supported Pd catalyst in aqueous medium. *J. Mol. Catal. A-Chem.* **260,** 115–120 (2006).
40. Rodrigo, E. *et al.* Reduced graphene oxide supported piperazine in aminocatalysis. *Chem. Commun.* **50,** 6270–6273 (2014).
41. Ren, M. *et al.* Electrocatalytic Oxidation of Formic Acid on Pd/Ni Heterostructured Catalyst. *J. Electrochem.* **18,** 515–520 (2012).
42. Yuan, R. *et al.* Ultrasensitive potentiometric immunosensor based on SA and OCA techniques for immobilization of HBsAb with colloidal Au and polyvinyl butyral as matrixes. *Langmuir* **20,** 7240–7245 (2004).
43. Ning, G., Lu-Yan, W., Wei-Min, X., Tian-Hua, L. & Qian-Li, J. Electrochemical Immuno-Biosensor for the Rapid Determination of Nuclear Matrix Protein 22 (NMP22) antigen in Urine Samples by Co (III) Phthlocyanine/Fe_3O_4/Au Collide Coimmobilized Electrode. *Chinese J. Anal. Chem.* **35,** 1553–1558 (2007).
44. Lee, M.-H. *et al.* Electrochemical sensing of nuclear matrix protein 22 in urine with molecularly imprinted poly (ethylene-co-vinyl alcohol) coated zinc oxide nanorod arrays for clinical studies of bladder cancer diagnosis. *Biosens. Bioelectron.* **79,** 789–795 (2016).
45. Han, T. *et al.* Gold nanoparticles enhanced electrochemiluminescence of graphite-like carbon nitride for the detection of Nuclear Matrix Protein 22. *Sensor. Actuat. B-Chem.* **205,** 176–183 (2014).

Acknowledgements

This study was supported by the National Natural Science Foundation of China (Nos 21375047, 21377046, 21405059, 21575050 and 21505051), the Science and Technology Plan Project of Jinan (No. 201307010), the Science and Technology Development Plan of Shandong Province (No. 2014GSF120004), the Special Project for Independent Innovation and Achievements Transformation of Shandong Province (No. 2014ZZCX05101), and QW thanks the Special Foundation for Taishan Scholar Professorship of Shandong Province (No. ts20130937) and UJN.

Author Contributions

D.W. and Q.W. conceived and designed the experiments. D.W. and Y.W. performed the experiments, analyzed the data and wrote the first draft of the manuscript. Y.Z., H.M., T.Y. and B.D. contributed substantially to revisions.

Additional Information

Competing financial interests: The authors declare no competing financial interests.

How to cite this article: Wu, D. *et al.* Sensitive Electrochemical Immunosensor for Detection of Nuclear Matrix Protein-22 based on NH_2-SAPO-34 Supported Pd/Co Nanoparticles. *Sci. Rep.* **6**, 24551; doi: 10.1038/srep24551 (2016).